”VICTOR BABEŞ” UNIVERSITY OF
MEDICINE AND PHARMACY TIMIŞOARA
FACULTY OF MEDICINE
DEPARTMENT OF UROLOGY
DEPARTMENT OF GASTROENTEROLOGY AND HEPATOLOGY

PhD THESIS

ELASTOGRAPHY IN THE DETECTION OF PROSTATE CANCER. ELASTOGRAPHIC GUIDED PROSTATIC BIOPSY. INTEGRATION OF ELASTOGRAPHIC DATA IN AN ARTIFICIAL INTELLIGENCE SYSTEM

ABSTRACT

Scientific Coordinator:
Prof. Univ. Dr. Ioan Sporea

PhD student:
Cosmin Ciprian Secășan

Timișoara

2024

Content

INTRODUCTION……1

1. GENERAL NOTIONS ABOUT PROSTATE CANCER….2
1.1 Incidence and epidemiology…….2
1.2 Risk factors……2
1.3 Pathological anatomy ……2
1.4 Histology of prostate cancer.....2
1.5 Prognosis of prostate cancer.....2
2. PROSTATE CANCER DIAGNOSIS……3
2.1 Detecting prostate cancer.....3
2.2 Histological diagnosis of prostate cancer ……3
2.3 Complementary examinations.....3
3.TREATMENT OF PROSTATE CANCER……3
3.1 Loco-regional and hormonal treatment……3
3.2 Systemic treatment: Chemotherapy……4
4. ULTRASONOGRAPHIC GUIDED PROSTATIC BIOPSY PUNCTURE…….4
4.1Method……4
4.2 Interpretation of biopsy results.....4
5. ELASTOGRAPHY OF THE PROSTATE.....4
5.1 Quasi-static elastography (Strain Elastography) SE.....4
5.2 Shear wave elastography (SWE).....5
6. ARTIFICIAL INTELLIGENCE IN ULTRASONOGRAPHY AND ELASTOGRAPHY.....5
7. RESEARCH OBJECTIVES.....5
8. ELASTOGRAPHY OF THE NORMAL AND PATHOLOGICAL PROSTATE….6
8.1 Motivation……6
8.2 Patients, material and methods……6
8.3 Results……8
8.4 Discussions.....8
9. ELASTOGRAPHY IN THE DETECTION AND DIAGNOSIS OF PROSTATE CANCER.....8
9.1 Motivation……8
9.2 Patients, Material and Methods……8
9.3 Results……9
10. IMPLEMENTATION OF ARTIFICIAL INTELLIGENCE IN PROSTATE CANCER DETECTION USING 2D-SWE ELASTOGRAPHY MEASUREMENTS.....9
10.1 Motivation.....9
10.2 Patients, Material and Methods.....9
10.3 Results.....11
11.THE USE OF ARTIFICIAL INTELLIGENCE IN THE MANAGEMENT OF PROSTATE CANCER RISK GROUPS……12
11.1 Motivation……12
11.2 Patients, Material and Methods……12
11.3 Results……12
12. ARTIFICIAL INTELLIGENCE-BASED METHOD FOR EFFICIENCY OF CANCER RISK GROUP MANAGEMENT BY COUPLING A FEATURE ATTENTION MECHANISM TO A DEEP ARTIFICIAL NEURONAL NETWORK..... 13
12.1 Motivation.....13
12.2 Material and methods……13
12.3 Results……14
13. CONCLUSIONS……14

Selective Bibliography……15

INTRODUCTION

Prostate cancer (PCa) is a public health problem worldwide. PCa is the most frequently diagnosed malignant tumor in adult men, and its incidence rate is continuously increasing [1]. PCa is the second leading cause of cancer death in men, after lung cancer. In the last 20 years, the application of screening methods by determining prostate specific antigen (prostate specific antigen - PSA), rectal examination (digital rectal examination - DRE) and transrectal ultrasound (transrectal ultrasound - TRUS) have significantly changed the way of detection, diagnosis and therapeutic approach to prostate cancer.

TRUS is a safe procedure that can provide effective evidence for PCa detection. TRUS, however, is a non-quantitative method that is associated with subjective measurements and largely depends on the ability of the physician performing the examination [2]. Although traditional transrectal grayscale ultrasonography is commonly used in PCa diagnosis and to guide biopsy, it is not sufficiently sensitive or specific for biopsy procedures. Biopsy protocols should be optimized to accurately detect PCa while reducing the number of prostate biopsy specimens and patient morbidity associated with biopsy [3]. A new ultrasonography technique proposed and currently used to guide prostate biopsies is elastography. PCa is stiffer than normal tissue due to its increased cellularity, an aspect that can often be detected on rectal examination [4]. Transrectal elastosonography has already been tested as feasible in guiding biopsies and useful for improving the detection of prostate lesions [5]. Shear Wave Elastography (SWE) represents a new imaging technique that offers the possibility of a quantitative assessment of the stiffness of the prostate tissue, expressed in measurement units (kiloPascals) [6], indicating the presence of PCa nodules and their location precise in the prostate gland, by differentiation from healthy tissue or benign lesions. Thus, SWE brings a considerable advantage in guiding prostatic biopsies and may reduce the number of biopsies required for PCa detection and diagnosis.

In recent years, the increasingly advanced and better performing medical imaging techniques have offered highly accurate data and measurements that can be integrated and quantified in matrices, networks and algorithms used in Artificial Intelligence systems. Medicine has started to use Artificial Intelligence (AI) more and more, coming to the aid of practitioners in establishing diagnoses and making therapeutic decisions, by analyzing a large number of parameters in a very short time and proposing management solutions and therapeutic behavior.

Thus, in this paper, we proposed as research topics, first of all, the assessment of the accuracy of PCa detection by transrectal prostatic biopsy guided by simultaneous standard ultrasonography in gray tones but also elastographic on a group of over 200 patients diagnosed with PCa and secondly correlation and integration of data obtained from elastographic measurements by subsequent reporting to the histopathological examination as a reference standard in a dynamic self-adaptive AI system, using Machine Learning (ML) and Deep Learning (DL) type classification algorithms. We consequently evaluated the reliability and reproducibility of the AI system in the detection of PCa with a view to further use in clinical practice, considering the very limited data published in the specialized literature until now.

1. GENERAL NOTIONS ABOUT PROSTATE CANCER

1.1 Incidence and epidemiology

Prostate cancer is one of the most common neoplasms in countries with high life expectancy, the risk increasing progressively with age. In the European Union, more than two million people live with prostate cancer, the most frequently diagnosed cancer among men [7].The incidence of clinically manifest cancer is extremely variable worldwide. It has been observed that geographic area and race have an important influence on incidence, with most new cases being recorded in North America and Scandinavian countries, while the condition is rarer in the Far East. Globally, prostate cancer ranked as the second most commonly diagnosed cancer in men, with approximately 1.4 million diagnoses worldwide in 2020, with subsequent increases in incidence to first place [8]. The current risk, for a man in a Western society, of developing microscopic prostate cancer during his lifetime is about 30%, the risk of developing clinical disease is about 10% and the risk of dying from this condition is about 3% [9].

1.2 Risk factors

*Genetic factors and environmental factors*causes the appearance of prostate cancer without, however, knowing the precise cause. Advanced age certainly has an influence on the risk factors and genetic changes that lead to prostate cancer. Family history can double the risk of prostate cancer in first-degree male relatives.

*Androgenic hormones*plays an important role in the initiation and progression of prostate cancer. Estrogen hormones act on normal and tumoral prostate tissue through estrogen receptors.

*Race and environmental factors.*There are numerous studies showing the higher incidence of prostate cancer in blacks compared to Caucasians and even Asians.

Eating. Epidemiological and biological studies have shown that increased caloric intake and excessive fat consumption are associated with an increased risk of developing prostate cancer.

Lifestyle. Excess weight and reduced physical activity, intense and early sexual activity, multiple sexual partners, history of sexually transmitted diseases, vasectomy, smoking are factors possibly associated with an increased risk of prostate cancer.

Genetic factors. Increased plasma levels of IGF-1 and cytochromes CYP17α and P450 3A4 polymorphisms involved in the biosynthesis and degradation of testosterone, respectively, seem to be associated with an increased risk [10].

1.3 Pathological anatomy

The zonal anatomy of the prostate, including the anterior, central, transitional and peripheral zones, is important to understand the origin of both benign hyperplasia and prostate cancer. Most cancers develop in the peripheral area. On the radical prostatectomy specimens, malignant tumors have an irregular outline, variable consistency and a whitish-gray or yellowish color. The initial focus expands centrifugally and progressively invades the prostatic parenchyma extending towards the prostatic capsule.

1.4 Histology of prostate cancer

Prostate cancer is usually an adenocarcinoma originating in the epithelial layer of the acini secretory, with multicentric histogenetic character and mixed histological appearance. Adenocarcinomas represent the vast majority of prostatic neoplasms. According to the degree of differentiation, they are classified into: G1 - very well differentiated, G2 - well differentiated, G3 - moderately differentiated, G4 - poorly differentiated and G5 - anaplastic (very poorly differentiated)

1.5 Prognosis of prostate cancer

Prognostic factors at the time of PCa diagnosis are represented by age, disease stage, degree of tumor differentiation (Gleason score), PSA value and to a lesser extent by serum acid phosphatase level and DNA ploidy.

2. PROSTATE CANCER DIAGNOSIS

2.1 Detection of prostate cancer

Early diagnosis or screening of PCa in asymptomatic men is achieved by: periodic assessment of PSA, digital rectal examination of the prostate (DRE) and transrectal ultrasound examination (TRUS). Routine evaluation of the suspected PCa patient will include: blood count, alkaline phosphatase, creatinine and PSA measurement.

2.2 Histological diagnosis of prostate cancer consists of:

Free-flow urinary cytology examination, from freshly emitted urine, which sometimes allows the discovery of class IV adenocarcinoma cells, therefore malignant.

Transrectal cytological aspiration with a simple needle. The study material consists of cells and not of tissue fragments.

*Prostatic biopsy puncture*involves the sampling of cylindrical fragments of prostatic tissue with a Tru-Cut needle, either transrectally, guided by rectal touch or ultrasound, or transperineal, guided by ultrasound with an endorectal transducer.

*Biopsy by TUR-P*simultaneously ensures both the resumption of normal urination and the sampling of fragments for histological diagnosis.

2.3 Complementary examinationsare represented by: multiparametric Nuclear Magnetic Resonance (NMRmp), plain X-ray; IV urography, Abdominal ultrasound, Retrograde uretero-pyelography, Pulmonary radiography, determination of acid and alkaline phosphatases, Lymphography and lympho-scintigraphy as well as bone scintigraphy.

3. TREATMENT OF PROSTATE CANCER

3.1 Loco-regional and hormonal treatment

Follow-up without treatment ("watchful waiting"). It is reserved for patients with Gleason score ≤ 4, with reduced life expectancy and/or with important comorbidities in whom palliation is the intention. It consists of evaluation every 6 months with clinical examination, DRE and serum PSA.

Active surveillance. It is addressed to patients with localized, low or intermediate grade PCa, with life expectancy > 10 years, with clinical reevaluation, DRE, PSA and periodic rebiopsies until the first sign of subclinical progression, when they will be integrated into curative treatment.

Surgery. Radical retropubic prostate-vesiculectomy, associated with pelvic lymphadenectomy, is the surgical treatment of choice in PCa.

Radiotherapy. *External radiotherapy*(RTEx) is used to treat localized forms of PCa. RTEx offers results comparable to radical prostatectomy in terms of survival at 5-10 years. Interstitial brachytherapy with palladium (103Pa) or radioactive iodine (125I) is used in patients with T1-2 tumors, PSA < 10 ng/ml, Gleason score < 6, as a boost after RTEx, or as a single therapy. Palliative radiation therapy, with total doses of 20-30 Gy, focuses in particular on bone segments with painful metastases, pathological fractures or signs of compression.

Hormonotherapy. Because PCa is an androgen-dependent tumor even in the initial stages, early hormone therapy is the treatment of choice in all stages of the disease.

Androgen deprivation. *Surgical castration*consisting of bilateral subcapsular orchiectomy is the "gold standard" for reducing circulating testosterone levels.

*Chemical castration*consists in the administration of pituitary gonadotropin hormone analogues or LH-RH analogues, which regulate the release of pituitary luteinizing hormone (LH) and consequently decrease testosterone production in the testicles.

*Blocking the testosterone receptor.*Steroidal and nonsteroidal antiandrogens block the entry of dihydrotestosterone (DHT), the active metabolite of testosterone, into the prostate cell nucleus. Total androgen blockade. In patients treated by surgical castration or with LHRH analogues, the combination of an antiandrogen can determine positive results in 30-40% of cases.

Estrogens.The main effect of estrogen administration in locally advanced and metastatic PCa is to block pituitary LH secretion with the consequent reduction of testosterone production from testicular Leydig cells.

3.2 Systemic treatment: Chemotherapy. Prostate cancer was initially recognized as unresponsive to chemotherapy, palliation of the symptomatic disease remaining its main goal [11].

4. ULTRASONOGRAPHICALLY GUIDED PROSTATIC BIOPSY

4.1 Method

Current indications for the need to perform a prostate biopsy are given by Total PSA increased, Free PSA < 20%, PSA velocity > 0.75 ng/ml per year, abnormal DRE, negative previous biopsies but after which there is still a clinical, biochemical or histopathological suspicion high for prostate cancer.

Anesthesia consists in the administration of a local anesthetic, currently being a standardized practice [12]. 10 ml of 1% lidocaine is injected using a long 22 gauge needle [13]. The anesthetic can be administered around the neurovascular bundle between the base of the gland and the seminal vesicles.

Antibiotic prophylaxis is necessary due to the risk of infection with microorganisms such as Escherichia coli, anaerobes and Gram-positive bacteria [14]. Post-biopsy infection rates without antibiotic prophylaxis are rated at 1 - 6%, which increases the potential for moderate to severe infections or even septicemia requiring hospitalization in 0 - 4% [15].

The overall complication rate of TRUS-guided prostate biopsy remains low. The main possible complications are: hematuria, hematospermia, acute urinary retention, persistent dysuria, fever or chills.

The biopsy technique consists in the transrectal sampling of fragments of prostate tissue under visualization and ultrasound guidance, using 18 Gauge Tru-Cut biopsy needles, the targeted prostatic regions being mainly the peripheral ones. The number of biopsies has increased from 6 fragments taken in the original sextant biopsy proposed and developed by Hodge [16] to 10 - 12 fragments representing the current accepted international standard, systematically harvested according to the number established by the protocol [17]. Current routine biopsy protocols do not provide for sampling from the inner part of the prostate because of the lower rate of occurrence and development, and therefore implicitly of detection of cancer in this region as well as its lower metastatic potential.

4.2 Interpretation of biopsy results

In the case of histopathological diagnosis of prostate cancer, the Gleason grading system is used, which establishes aggressiveness and is essential for management and risk stratification. A five-point scale is used to grade the cellular architecture in a biopsy fragment from very well differentiated to undifferentiated. The Gleason score is obtained by summing the two most common degrees of anatomopathological differentiation, primary and secondary, determined in the sampled fragments, or by multiplying by 2 the only grade identified, if applicable. The combined score ranges from 2 to 10.

5. ELASTOGRAPHY OF THE PROSTATE

5.1 Quasi-static elastography (Strain Elastography) SE

Quasi-static elastography is based on the analysis of the deformation of the tissue in a certain region, generated by the induction of a mechanical stress given by its successive compression and decompression with the transducer by the operator. It is assumed that the deformation is uniform in space and in intensity [18]. The subsequent displacement of the tissues is tracked between pairs of ARFI - Acoustic Radiation Force Impulse echo frames, and the deformation is calculated from the axial gradient of the displacements. Under an equal amount of applied stress, a stiff region undergoes less deformation than the surrounding softer tissue. Using a color map to encode the different magnitudes of stress, by

comparing the pre- and post-compression images, a two-dimensional stress image called an “elastogram” is obtained, which can be translucently superimposed over the conventional B-mode ultrasound image displayed simultaneously, helping to evaluation of the spatial relationship between the ultrasound image and the elastographic data. Quantitative measurements of elasticity cannot be obtained because the local degree of stress is unknown. Therefore, strain elastography is a qualitative technique in which the relative stiffness differences in the tissue being studied are displayed.

5.2 Shear Wave Elastography (SWE)

Unlike quasi-static elastography, Shear Wave Elastography (SWE) when evaluating the prostate does not require compression on the rectal wall to produce elastograms. SWE is based on measuring the velocity of shear waves propagating through tissues [19]. This technique provides a quantitative map of the elastic properties of soft tissues in real time, displayed in either kiloPascals or meters per second. The transducer automatically generates an acoustic radiation force using a special "supersonic" speed that moves multiple focus points following the Mach cone principle. The tissue is then mechanically excited by the Mach cone impulse to generate small, localized tissue displacements of 1-10 mm. These displacements are tracked using a shear wave propagation velocity calculation system, Young's modulus, determining the tissue's quantitative stiffness, expressed in kPa. Young's modulus is defined by the equation $E = \sigma/\varepsilon$, where σ is the applied stress and ε represents the deformation produced.

6. ARTIFICIAL INTELLIGENCE IN ULTRASONOGRAPHY AND ELASTOGRAPHY

Artificial intelligence (AI) is defined and characterized by the ability of digital technology to simulate human intelligence, at least in partial domains such as decision making[20]. It includes Machine Learning as its main subfield and this in turn includes Deep Learning as a subfield.

In the medical field, the interpretation of medical images is inherently a stage of data processing where AI can be implemented.There are many opportunities to implement AI to optimize the screening process for PCa, such as improving the detection rate by ultrasound and MRI, reducing inter-observer variability among radiologists, and assisting pathologists in identifying and classifying cancer on histopathological images. As elastography has gradually been used as a complement to conventional ultrasonography, providing information on elasticitytissues, there is a growing trend in AI-based elastographic image analysis applications. By eliminating the variability between examiners, the developed models allowed increasing the accuracy of image interpretation and implicitly the diagnosis based on elastography.

7. RESEARCH OBJECTIVES

The experimental part of this thesis was structured in five distinct chapters, including five different studies, in which I proposed as main objectives:

1) Elastography of the normal prostate and prostate adenoma
2) Elastography of the prostate with suspicion of prostatic adenocarcinoma
3) Elastographically guided prostatic biopsy
4) Acquisition of images and comparative elastographic measurements between various aspects of prostate tissue: normal, adenomatous and malignant
5) Acquisition of standard ultrasonographic and elastographic images in cases with suspected prostatic adenocarcinoma, which then underwent TRUS-guided biopsy targeting the areas that presented the most imaging aspects suggestive of malignant transformation

6) Integrating data obtained from quantitative elastographic measurements, using the 2D-SWE technique, into an artificial intelligence system in order to create a high-accuracy prostate cancer detection method

The first two studies were focused on evaluating the contribution of elastography in the detection and diagnosis of prostate cancer, and the remaining three on the implementation of an Artificial Intelligence system based on Machine Learning and Deep Learning technologies, as well as on the creation of a neural network to analyze the data provided by SWE elastography used in the determination of prostate gland pathology.

8. ELASTOGRAPHY OF THE NORMAL AND PATHOLOGICAL PROSTATE

8.1 Motivation.

This first study proposed to approach a topic of great scientific relevance, namely the optimization of prostate cancer diagnosis with the help of this new ultrasonographic method, prostatic sonoelastography. At present, the main method of positive diagnosis, definitely, in prostate cancer, is the prostatic biopsy guided by transrectal ultrasonography. Elastography brings a considerable advantage in the imaging guidance of the prostate biopsy puncture, clearly highlighting the regions of neoplastic tissue and offering the possibility of reducing the number of fragments to be harvested necessary for the biopsy, thus increasing the effectiveness of the procedure but also reducing the operative times and the rate of possible intraoperative and postoperative complications.

8.2 Patients, material and methods

100 patients were initially elastographically examined, between October 2016 and March 2018, divided into 2 groups: the first group included 63 patients with normal PSA values, between 0 and 4 ng/ml and the second group of included 37 patients with elevated serum PSA values, above 4 ng/ml. The patients in the second group had a mean age of 65 years (range 44 - 86 years), with a mean serum PSA value of 11.13 ng/ml (range 4.5 - 28.3 ng/ml). Group 1 included patients with normal PSA, aged between 35 - 85 years, with or without lower urinary tract symptoms. Group 2 included patients aged between 44 and 86 years with PSA > 4ng/ml with or without positive rectal palpation, in the case of positive palpation, with one or more palpable tumor nodules. The exclusion criteria had as considerations conditions or physiological states with the possible presence of pelvic-perineal inflammation: acute or chronic prostatitis, acute epididymitis, orchiepididymitis, acute urethritis, acute, subacute cystitis, as well as the presence of recent or chronic recurrent urinary tract infections . The elastographic techniques used were: Shear Wave Elastography SWE (dynamic, operator independent; the device emits acoustic waves that deform the tissues, measuring their propagation speed and appreciating the tissue deformation. The measurements are quantitative) and Strain Elastography SE (quasi-static, operator dependent; the examiner applies repetitive pressure to the area of interest.Measurements are qualitative). The equipment used to perform elastography included two ultrasound machines with different elastographic modules, one with SWE and one with SE, respectively AIXPLORER model RAP2102LM-SSI from SuperSonic Imagine, with the SuperEndocavity SE12-3 endocavity probe and LOGIQ E9 model 5205000 from General Electric, with the IC5-9 endocavitary probe with frequencies between 3 and 10 MHz.

We reproduce below some of the relevant elastographic acquisition images obtained:

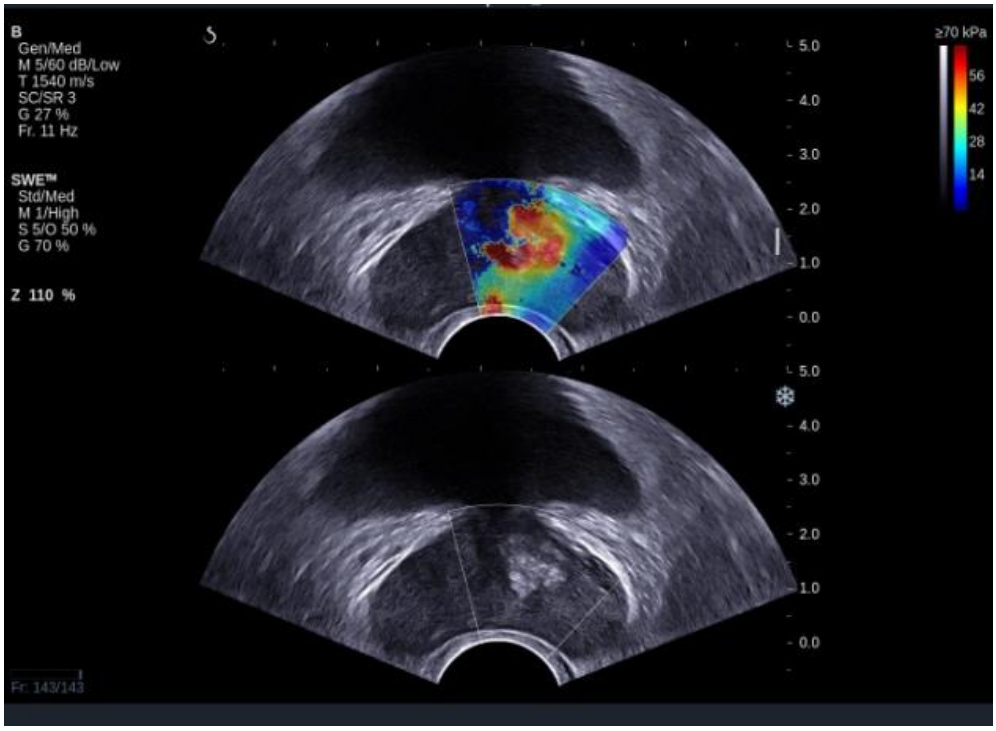

Fig.1 Area of calcification in the middle portion of the right prostatic lobe, with increased density and stiffness, highlighted elastographically by staining with shades from orange to intense red

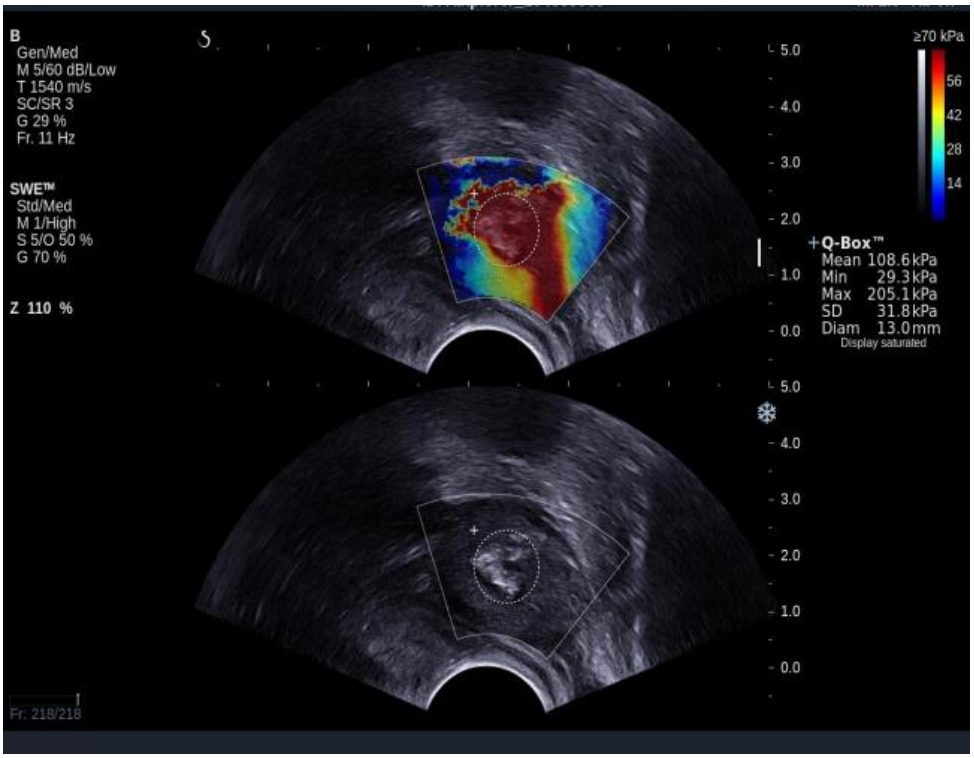

Fig.2 Suspected patient with prostatic adenocarcinoma. Intense red staining indicating an area of increased elastographic density, most likely malignant

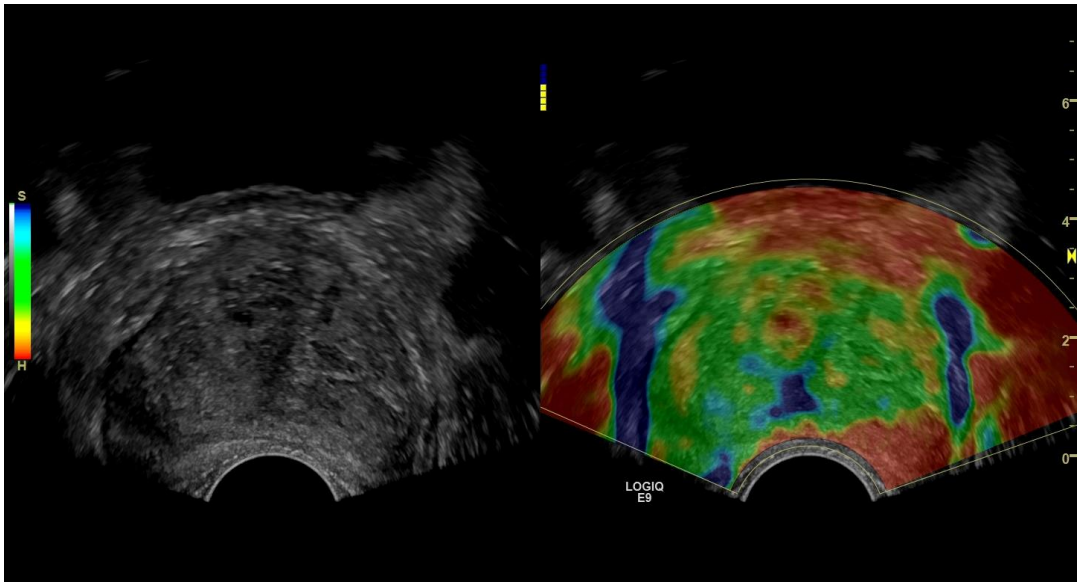

Fig.3 Prostate adenoma highlighted by the SE technique. The prostate is relatively homogeneous in terms of tissue consistency, without areas of increased density that in this case would produce a signal in shades of blue, corresponding to the specific coding of the strain elastography technique

8.3 Results

We obtained a batch of 526 elastographic images characteristic of normal, adenomatous and neoplastic prostate tissue, of which 410 by the SWE technique and 116 by the SE technique, in a significant proportion regarding the relevance of elastographic examinations addressed to the prostate.

8.4 Discussions

The normal prostate gives a homogeneous appearance with elastographic values usually below 30 kPa by the SWE technique. In prostate adenoma, the central and transitional zones become heterogeneous and dense, harder, with increased elastogram values. Prostate cancer offers, especially in the peripheral area, much increased elastographic values, mostly well over 35 kPa, values even over 200 kPa being obtained in cases with typical malignant hard nodules.

9. ELASTOGRAPHY IN THE DETECTION AND DIAGNOSIS OF PROSTATE CANCER

9.1 Motivation

The aim of this study was to evaluate the false-negative rate of elastographically guided 12-slice prostate biopsy. We also took into consideration the suspicious characteristics for PCa of the patients that may affect the detection rate.

9.2 Patients, Material and Methods

We included in the study only patients diagnosed with prostate cancer by biopsy puncture systematized in 12 fragments guided by transrectal ultrasound, initially selected according to the elevated serum PSA level and according to clinical signs of malignancy present on positive rectal swabs, palpable prostatic nodules or regions of indurated tissue, with increased consistency on palpation, in which, prior to performing the systematic biopsy puncture, we evaluated the entire prostate gland elastographically using the 2D-SWE technique. A total of 30 selected patients were prospectively included in the study, with an average age of 60.81 years, age range between 47 and 75 years, with serum PSA between 4.5 and 52 ng/ml with or without suspicion of prostate cancer on rectal palpation. We did not include in the study patients with a history of prostate biopsy or endoscopic or classical

surgical treatment addressed to prostatic pathology. Also, patients who had a recent pathological history of prostatitis, adenomyitis, lower urinary tract infections in the last month were not considered eligible. We performed elastographic measurements related to the prostatic regions targeted for the systematic puncture and took into account the presence of possible suspicious nodular regions located outside them. The study period was between February 2017 and May 2018. The biopsies were performed in the Urology Clinic of the Timișoara County Emergency Clinical Hospital, in collaboration with the Gastroenterology Clinic. All patients included in the study subsequently underwent surgical treatment, i.e. radical retropubic prostatectomy. The age of the patients, the prostatic volume measured preoperatively by ultrasound, the serum PSA value, the PSA density, the Gleason score obtained preoperatively during the biopsies and postoperatively, after the prostatectomy, were taken into account. Prostatic biopsy puncture was performed under local anesthesia, with 10 ml xyline 1% or lidocaine, the local anesthetic being injected at the base of the seminal vesicles, bilaterally postero-laterally in relation to the prostate gland. The machine used to perform the punctures and elastographic correlation of the areas suspected of prostate cancer was the SuperSonic Image SE12-3 MHz Transrectal Probe AIXPLORER, on which an endocavitary "endfire" puncture guidance system manufactured by CIVCO was applied Medical Solutions, reusable by sterilization. The puncture gun used was the BARD MG1522 Magnum reusable, dual spring system, with biopsy depth settings of 15 and 22 mm, in combination with the BARD Magnum Needle 18G or compatible.

9.3 Results

The Gleason score obtained after the histopathological examination of the excision pieces after prostatectomy remained the same in 23 patients (76.6%), increased in 5 patients (16.6%) and decreased in 2 patients (0.06%), in comparison with the Gleason score obtained after the preoperative histopathological examination corresponding to transrectal biopsy punctures. Of the total number of patients, 12 had preoperative PSA between 4 and 10 ng/ml. In 4 of them, a difference was found between the initial Gleason score and the one after radical prostatectomy. The other 3 patients in whom the Gleason score differed had PSA between 10 and 15 ng/ml. The Gleason score was not different in any of the 9 patients with PSA > 15 ng/ml. We found the increase in the rate of correct diagnosis correlated with the increase in the serum PSA value, but also with the reduction in prostate volume.

10. IMPLEMENTATION OF ARTIFICIAL INTELLIGENCE IN PROSTATE CANCER DETECTION USING 2D-SWE ELASTOGRAPHY MEASUREMENTS

10.1 Motivation

Our primary objective was to design an artificial intelligence system capable of predicting prostate cancer using data obtained from shear wave elastography of the prostate, then comparing it with data collected from histopathological examination of prostate biopsy specimens, considered reference standard.

10.2 Patients, material and methods

We conducted a prospective study, which included more than 350 patients initially presented for consultation in our specialty outpatient clinic, later scheduled for prostate biopsy guided by transrectal ultrasound, for suspected prostate cancer, between January 2017 and November 2019. Among of the initially included patients, 223 were diagnosed and confirmed with PCa following histopathological examination performed after prostate biopsy. We used the following inclusion criteria for patient selection: at least a total prostate-specific antigen (PSA) value above 4 ng/ml and/or an abnormal digital rectal examination, raising the suspicion of prostate cancer. Subsequently, we applied the following exclusion criteria: history of prostate cancer, history of surgical or endoscopic lower urinary tract procedures, history or recent signs of acute or subacute prostatitis. Ultrasonographic examination was combined, including conventional transrectal ultrasound and SWE elastography, for direct biopsy immediately after elastographic image acquisition. The prostate was divided into

twelve circular target areas of 5 mm diameter, six peripheral and six para-urethral, approximately 1 cm apart. Each area was initially assessed for the presence of hypoechoic lesions on grayscale ultrasound, which was followed by two-dimensional shear wave elastography.

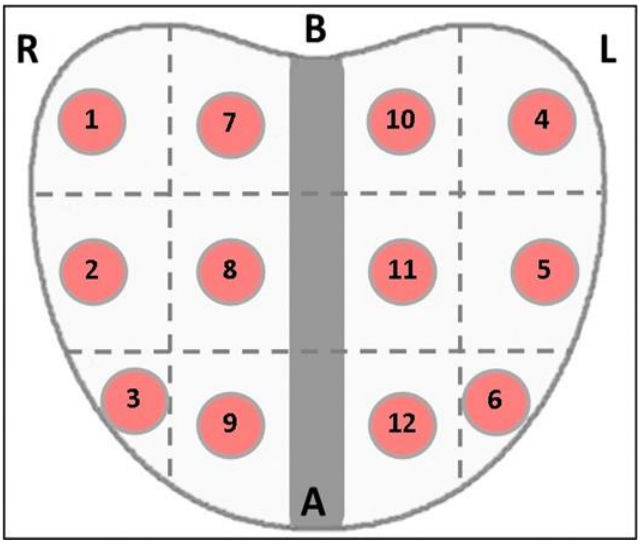

Fig. 4 Prostate divided into twelve target areas, resulting in a total of twelve biopsy fragments approximately 1 cm apart. Each target area and tissue fragment corresponds to a region evaluated with SWE measurements before biopsies were taken (R = right, L = left, B = base, and A = apex).

We constructed the data set by considering the measurement values in kPa for each biopsy fragment. For the set analysis, we implemented three machine learning classification algorithms, namely logistic regression, a decision tree classifier, and a fully connected feed-forward deep neural network [21].

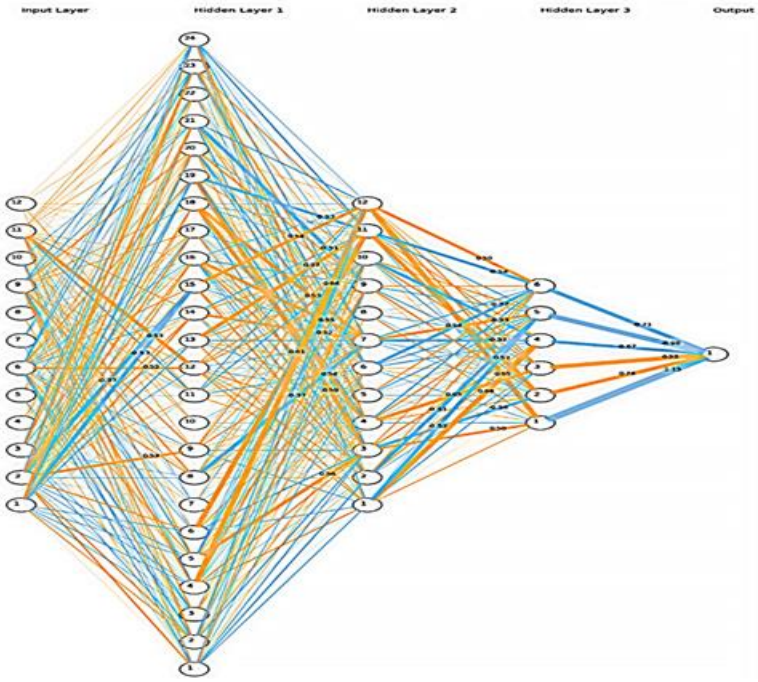

Fig. 5 Deep learning model visualization. The neurons represented by the small circles are numbered from bottom to top in each layer, in ascending order. The first layer is the input layer with the elasticity values. The other four processing layers (three hidden and one output) are described in the table V. Activation weights are marked with a bold line.

We used the receiver operating characteristic curve (ROC) created by graphically representing the true positive rate in relation to the false positive rate at different threshold values as a performance evaluation measure [22]. We used for normalized units the area under the curve (AUC), which is equal to the probability that a classifier will classify a randomly chosen positive instance better than a randomly chosen negative instance. In addition, we calculated sensitivity and specificity, as these are statistical measures of the performance of a binary classification test. Cross-validation was performed, using the "k-fold" procedure, which divides all samples into groups of samples, called "folds", of equal size. The prediction function was learned using the sample groups, and the left-out group was used for testing.

10.3 Results

Of the total of 356 patients examined, who were evaluated in our protocol, a number of 223 were confirmed to have prostate cancer. By comparing the results of the three AI systems, we obtained the highest accuracy with the neural network classifier, namely AUC = 0.94, followed by logistic regression with AUC = 0.88 and decision tree with AUC of 0.78. This is mainly due to a slight imbalance between positive and negative cases, with a higher proportion of positive prostate cancer cases in the dataset. For the neural network, the final accuracy values were: loss = 0.0513, mean absolute value = 0.1272, and root mean square error = 0.0513. For the test set, we obtained mean absolute error = 0.12 for ExHP. To solve the imbalance, we used the SMOTE oversampling strategy [23], but only for the training set, so that the newly generated samples do not influence the model prediction. After applying SMOTE, we obtained a perfectly balanced dataset with 290 entries in the training data. By retraining the deep neural network classifier, the AUC improved slightly to reach AUC = 0.95.

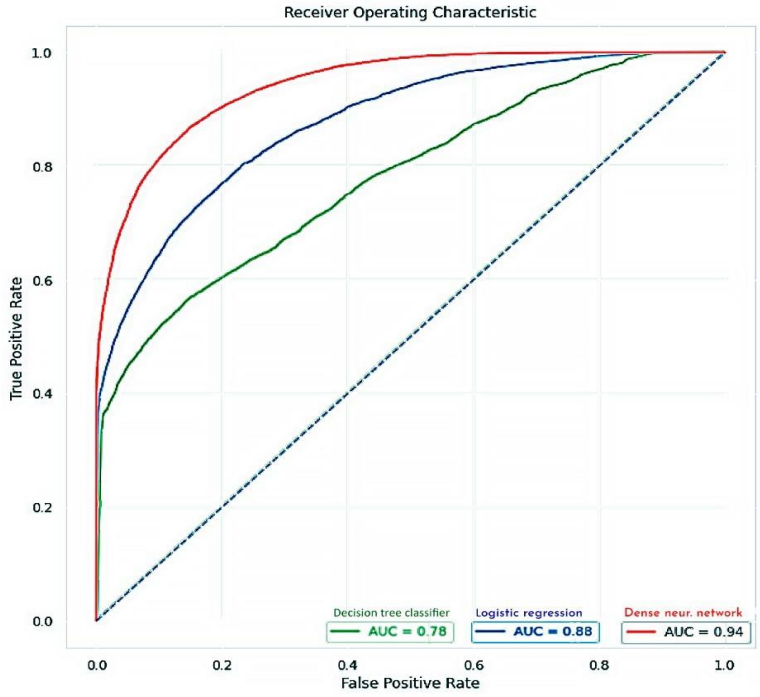

Fig. 6. ROC curves of the three systems used for prediction: logistic regression (trained with gradient descent instead of ordinary least squares, marked in blue; AUC = 0.88), decision tree classifier (using the ID3 algorithm, marked in green; AUC = 0.78) and the dense neural network (with three hidden layers, marked in red; AUC = 0.94).

Our intelligent system ultimately provided a high level of accuracy but, given the relatively moderate size of the data set, did not allow us to omit systematic randomized biopsy in favor of SWE targeted biopsy.

11. THE USE OF ARTIFICIAL INTELLIGENCE IN THE MANAGEMENT OF PROSTATE CANCER RISK GROUPS

11.1 Motivation

Our objective was to design and use a novel artificial intelligence system capable of determining a prostate cancer prognostic score using data obtained from prostate SWE elastography measurements, in subsequent comparison with data from histopathological examination of prostate biopsy specimens, selecting only cases with positive findings of prostate cancer.

11.2 Material and methods

We used the database from the previous study, including only patients with a positive histopathological result for PCa, and with Gleason classification and grading on each fragment taken, in the case of positive fragments. We created an AI system based on a custom-designed neural network classifier, adapted to patient data sets collected through highly specialized medical screening, in our case 2D-SWE measurements, with subsequent validations. We further processed this data set to fill in fragments with missing values with the neutral value 22, the average reference value of SWE measurements in normal or benign tissues. To design our supervised AI multi-class classifier, we had to define the target classes following the needs of clinical diagnosis. Therefore, we divided the patients in the database into three well-balanced categories: Risk 0 or low, Risk 1 or medium, and Risk 2 or high. The first category consists of patients with Gleason score less than 7 and corresponding fragment values, the Risk 2 category is represented by patients with Gleason score greater than 7 and corresponding fragment values. We paid special attention to patients with a Gleason score of exactly 7 from variants of 3+4 or 4+3 degrees of differentiation, determined by the anatomopathologist. These are initially located in risk category 1, but after further processing can be further distributed into a low or high risk category, providing a clearer prognosis and a new risk category placement beyond the currently established accepted stage. We noticed that for a correct characterization of cases with Gleason score 7, it is necessary to introduce a new index, considering the fragment values. We called the new score "Gleason-Fragments Index (GFI)". We calculated this combined Gleason-Fragment score using the following formula:

$$GFI = \frac{(\mathbf{Frag1} + \mathbf{Frag2} + \mathbf{Frag3} + \mathbf{Frag4} + \mathbf{Frag5} + \mathbf{Frag6} + \mathbf{Frag7} + \mathbf{Frag8} + \mathbf{Frag9} + \mathbf{Frag10} + \mathbf{Frag11} + \mathbf{Frag12}) / \mathbf{12}}{\boldsymbol{Gleason\ Score}}$$

The GFI is calculated by taking the average of the fragments and then further dividing it by the Gleason Score. To be able to use it in practice for Risk 1 patients, we need to calculate a threshold value for GFI. The threshold value is calculated by taking the average of the highest GFI index calculated for patients at risk 0 and the lowest GFI index observed for patients at risk 2. After performing experiments on our data set, we obtained a value of 11 for this threshold. This observation completes our study and allows us to add an additional rule-based layer to our neural network for correctly determining Risk 1 patients where we have Gleason score 7 in both 3+4 and 4+3 combinations. Therefore, the neural network receives two inputs, namely the Gleason score and the new GFI index.

11.3 Results

To verify the statistical significance of the GFI index we further calculated the p-value (p-value) of the level of statistical significance for the correlation between the fragment values considered together with the Gleason score and the histopathological examination. The calculated p-value is 0.00235 and since $p<0.01$, the statistical association is significant with approximately 99% confidence. The artificial neural network was implemented in Python programming language using Keras and Tensorflow libraries. It was constructed with two inputs namely the Gleason score and the GFI index. It has three hidden layers, one with 8 neurons, the second with 4 neurons and the third also with 4 neurons. For training, we used K-fold validation with K of 4 samples. After the back-propagation training step, we obtained

the following values: Sensitivity for risk class 0: 0.80, Specificity: 0.68; Sensitivity for class 1: 0.84, Specificity: 0.70; Sensitivity for class 2: 1.00, Specificity: 0.78.

12. ARTIFICIAL INTELLIGENCE-BASED METHOD FOR EFFICIENCY OF CANCER RISK GROUP MANAGEMENT BY COUPLING A FEATURE ATTENTION MECHANISM TO A DEEP ARTIFICIAL NEURAL NETWORK

12.1 Motivation

In this last study, we proposed a method to streamline the management of risk groups in cancer by coupling a feature attention mechanism with a deep supervised artificial neural network. We used data sets from patients with two different neoplastic pathologies, pulmonary and prostatic, collected from two different clinics, the one of thoracic surgery and the one of urology, from two different health units.

12.2 Material and methods

For the implementation of the method in the study of risk groups in prostate cancer, we used a set of data collected in the Urology Clinic of the Emergency Clinical County University Hospital in Timișoara. This data set included 138 patients diagnosed by TRUS-guided prostate biopsy and 2D-SWE with prostate cancer with the histopathological type of prostate adenocarcinoma, with 20 associated characteristics for each individual: age, PSA, prostate volume, results of scans by rectal smear, positive or negative for prostate cancer nodules, histopathological examination as reference standard, Gleason score according to histopathological examination results, number of prostate biopsy fragments, positive prostate cancer fragments after histopathological evaluation, maximum extent of tumors, and most importantly SWE measurements in kPa for each of the biopsy fragments. To compile the data set, we grouped patients according to Gleason scores determined by histopathological examination. We considered only those patients with Gleason scores equal to 7, representing the intermediate risk group in the prostate cancer risk group classification system for localized tumors (EAU 2019). If the patient had a Gleason score of 3 + 4 = 7 or 4 + 3 = 7 (ISUP 2 or 3), and the mean of all fragments was less than the mean of M.min (the lowest mean of the 12 fragments) and M.max (the highest average of the 12 fragments), then the risk would be 1. If this average of all fragments were greater than the average of M.min and M.max, and the Gleason score would still be 7 (3 + 4 = 7 or 4 + 3 = 7) or greater, the risk would be 2. In cases where the Gleason score value is less than 7, the risk is 0. After classifying patients according to their risk of colon cancer prostate, we obtained the following result (figure 7):

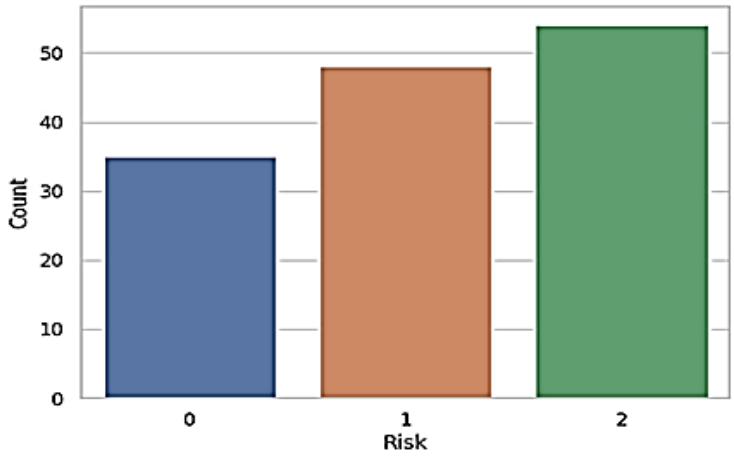

Figure 7. Number of patients with risk levels of 0, 1, or 2 in the urology dataset

Since the patient management risk value can take values from 0 - 2, it is a multi-class classification. The value 0 represents a patient who is most likely to be at low risk, 1 denotes that the patient tends to be at intermediate risk, and 2 signifies that the patient is most likely suffering from an advanced form of the disease. Based on the 2D-SWE measurements, we determined the value in kPa for each fragment. The SWE feature did not include a fixed number of relevant prostate tissue elasticity/density values. We fell to a common denominator by filling in all the fragments until we had no more irrelevant or missing values in the table of SWE measurement values. When the relevant values in the data set were exhausted, we added the average value of 22 to the remaining incomplete fragments.

12.3 Results

We trained a neural network with four deep layers and evaluated the performance of the model using four-fold cross-validation with the binary classification task. We designed from scratch a six-layer deep neural network for the urology dataset using, again, four-fold cross-validation for the multi-class case. After training the dataset that included only the features with positive impact relevant to our analysis, we were able to increase its accuracy by 20% compared to the instance where we used the entire dataset. The accuracy value obtained from using the LIME method and applying the attention mechanism on both datasets was approximately 80%. In the case of multiple classes, the result was even better. Risk 1 patients were under 50 years of age, so they fell in the middle of the volume of patients with intermediate risk of prostate cancer. To extend the ROC-AUC performance feature to multiclass classification for Risk 0 and Risk 2, representing the most interesting clinical cases, we used a One-vs-Rest (OvR) approach. Therefore, a separate ROC curve was plotted for each class against all other classes, effectively treating the multi-class problem as a multiple binary classification problem. Following the obtained result, we can state that the developed model worked very well in the case of the multiple class as well as on a larger volume of information. The results obtained before using the developed method were: Accuracy 63.81%, Sensitivity 50.01% and Specificity 75.76%, and after, 78.18%, 54.55% and 99.97% respectively

13. CONCLUSIONS

1. 2D-SWE elastography, in combination with standard B-mode ultrasonography, is a reliable, reliable method, and of considerable utility in the imaging study of the prostate, differentiating potentially malignant lesions from benign lesions and normal tissue with reasonable accuracy.
2. 2D-SWE elastography can improve the results of echo-guided prostatic biopsy puncture, by targeting suspicious lesions and can thus encourage the performance of strictly elastographically guided transrectal prostatic biopsies, limiting the number of tissue fragments harvested, reducing morbidity, risks and intraoperative complications.
3. By implementing Artificial Intelligence systems in the processing of data obtained from SWE examinations, the diagnostic and prediction procedures in prostate cancer can be significantly simplified.
4.Our AI system provided a high level of accuracy, but given the relatively moderate size of the datasets, we did not completely omit systematic prostate biopsy in favor of strictly targeted SWE biopsy.
5. Considering the encouraging results obtained during the studies included in this paper, we consider it necessary to continue our research in the field of integration and analysis of relevant clinical data with the help of AI.

Selective Bibliography

1. Jemal, A. et al. Global cancer statistics. CA: a cancer journal for clinicians 61, 69–90, doi:10.3322/caac.20107(2011).
2. Bjurlin, MA et al. Optimizing baseline prostate biopsy in clinical practice: sampling, labeling and sample processing. Journal of urology 189, 2039–2046, doi:10.1016/j.juro.2013.02.072(2013).
3. Rodriguez, LV & Terris, MK Risks and complications of transrectal ultrasound. Current Opinion in Urology 10, 111– 116, doi:10.1097/00042307-200003000-00011(2000).
4. Konig, K. et al. Initial experiences with real-time elastography-guided biopsies of the prostate. Journal of urology 174, 115–117, doi:10.1097/01.ju.0000162043.72294.4a(2005).
5. Sumura, M. et al. Initial evaluation of prostate cancer with real-time elastography based on staged pathological analysis after radical prostatectomy: a preliminary study. International journal of urology: the official journal of the Japanese Urological Association 14, 811–816, doi:10.1111/j.1442-2042.2007.01829.x(2007).
6. Franchi-Abella, S., Elie, C. & Correas, JM Ultrasound elastography: advantages, limitations and artifacts of different techniques in a phantom study. Diagnostic and Interventional Imaging 94, 497–501, doi:10.1016/j.diii.2013.01.024(2013).
7. Van Poppel, H et al. Prostate Cancer: Recommendations to lower the risk and mortality of the most frequent cancer in men. European Association of Urology. 2018. Accessible at https://uroweb.org/wp-content/uploads/EAU_WhitePaper_PCa_final.pdf (last accessed September 2020)
8. Culp, MB, et al. Recent Global Patterns in Prostate Cancer Incidence and Mortality Rates. Eur Urol, 2020. 77: 38. https://pubmed.ncbi.nlm.nih.gov/31493960/
9. Etzioni R, Legler JM, Feuer EJ, et al. Cancer surveillance series: interpreting trends in prostate cancer-part III: quantifying the link between population prostate-specific antigen testing and recent declines in prostate cancer mortality. J Natl Cancer Inst. 1999;91:1033–1039. [PubMed] [Google Scholar]
10. Chen TC, Sakaki T, Yamamoto K, Kittaka A. The roles of cytochrome P450 enzymes in prostate cancer development and treatment. Anticancer Res. 2012 Jan;32(1):291-8.
11. Miron L. Prostate cancer. In: Bild E, Miron L, eds. Cancer therapy – a practical guide. Iasi: Tehnopres Publishing House, 2003:288-289
12. Kravchick S, Peled R, Ben Dor D, Dorfman D, Kesari D, Cytron S. Comparison of different local anesthesia techniques during TRUS-guided biopsies: a prospective pilot study. Urology 2005;65:109–13.
13. Turgut AT, Dogra VS. Transrectal prostate biopsies. In: Dogra V, Saad W, eds. Ultrasound guided procedures. New York, NY: Thieme; 2009. pp. 85–93.
14. Webb NR, Woo HH. Antibiotic prophylaxis for prostate biopsy. BJU Int 2002;89:824–8.
15. Ghani KR, Dundas D, Patel U. Bleeding after transrectal ultrasonography-guided prostate biopsy: a study of 7-day morbidity after a six-, eight- and 12-core biopsy protocol. BJU Int 2004;94:1014–20.
16. Hodge KK, McNeal JE, Terris MK, Stamey TA. Random systematic versus directed ultrasound guided transrectal core biopsies of the prostate. J Urol 1989;142:71–4.
17. NHS Cancer Screening Programmes. Undertaking a transrectal ultrasound guided biopsy of the prostate. PRCMP Guide no. 1. Sheffield, UK: NHS Cancer Screening Programmes; 2006.
18. Aigner F, Pallwein L, Junker D, Schäfer G, Mikuz G, Pedross F, et al. Value of real-time elastography targeted biopsy for prostate cancer detection in men with prostate specific antigen 1.25 ng/mL or greater and 4.00 ng/mL or less. J Urol 2010;184(3):913—7.
19. Bercoff J, Tanter M, Fink M. Supersonic shear imaging: a new technique for soft tissue elasticity mapping. IEEE Trans Ultrasound Ferroelectr Freq Control 2004;51(4):396—409.
20. Hamet, P.; Tremblay, J. Artificial intelligence in medicine. Metabolism 2017, 69, S36–S40. [CrossRef]
21. **C.Secasan, D.Onchis, R.Bardan, A.Cumpanas, D.Novacescu, C.Botoca, A.Dema, I.Sporea Artificial Intelligence System for Predicting Prostate Cancer Lesions from Shear Wave Elastography Measurements Curr. Oncologist 2022, 29(6), 4212-4223;https://doi.org/10.3390/curroncol29060336 - 10 Jun 2022**
22. Brown, CD; Davis, HT Receiver operating characteristics curves and related decision measures: A tutorial. Let's call. Intel. Lab. Syst. 2006, 80, 24–38. [CrossRef]
23. **Darian M. Onchis, Flavia Costi, Codruta Istin, Ciprian Cosmin Secasan, Gabriel V. Cozma. Method of Improving the Management of Cancer Risk Groups by Coupling a Features-Attention Mechanism to a Deep Neural Network Appl. Sci. 2024, 14(1), 447;https://doi.org/10.3390/app14010447 - 04 Jan 2024**